Thermodynamic Nature of Monodisperse Polystyrene in Mixed Solvent of Cyclohexane and Antisolvent Carbon Dioxide Using Synchrotron Small-Angle X-ray Scattering

Dan Li, Zhimin Liu, Buxing Han,* Guanying Yang, and Liping Song

Center for Molecular Science, Institute of Chemistry, The Chinese Academy of Sciences, Beijing 100080, P. R. China

Jun Wang and Baozhong Dong

Institute of High Energy Physics, The Chinese Academy of Science, Beijing 100039, P. R. China

Received August 9, 2002; Revised Manuscript Received October 28, 2002

ABSTRACT: The synchrotron small-angle X-ray scattering (SAXS) technique has been used to study the effect of the antisolvent CO_2 on the thermodynamic properties of polystyrene (PS)/cyclohexane (CH) solutions at 34.5 °C and at pressures up to 30.0 bar. The molecular weights (M_w) of the monodisperse PS are 3600, 22 400, 84 000, 176 000, and 341 000. The cloud point pressures of the solutions at different solution concentration are also determined. The SAXS results show that the intramolecular radius of gyration (R_g) decreases with approaching cloud point pressure due to the increasing polymer−polymer interaction. At different antisolvent CO_2 pressure, there is an exponential relationship between R_g and M_w, and the exponents change from 0.5 to 0.341 with the pressure changing from 0 to 30 bar, which means that the shape of the PS chain changes from random coil to nearly globular. The intermolecular correlation length (ξ) increases dramatically as the phase separation boundary is approached, and it is 7 times larger than R_g. Near the phase separation boundary, the thermodynamic fluctuations in ternary systems lead to the formation of distinct microdomains, representing interpenetrating of macromolecules, and dramatic increase of the intermolecular correlation length.

Introduction

The relationship between polymer chain structure and its environment changing has been subject of interest for several decades.[1−8] Experimental observations of protein denaturation resulting from changes in solvent environment such as temperature, ionic strength, or acidity provided the first evidence of a structural transition in a macromolecule. The transition was measured through changes in the conformational dependent properties of the molecule: biological activity, optical rotation, UV absorption, and solution viscosity. The advent of scattering techniques such as laser light scattering (LS),[9] small-angle neutron scattering (SANS),[10] and small-angle X-ray scattering (SAXS)[11] has allowed polymer microstructure to be experimentally observed and compared with evolving theoretical descriptions of polymer conformation. The vast majority of these studies have considered polymers in liquid solvents or in blends. Conveniently, these work has laid the foundation for similar studies in supercritical fluids (SCF) solvents, as is evidenced by a publication by Luna-Barcenas et al.[12] which describes the use of Monte Carlo simulations to investigate the polymer chain conformation as a function of distance from a phase boundary. SCF solvents allow the response of a polymer to its environment to be measured by a very different type of perturbation in solvent quality: pressure. Several groups have initiated SANS and dynamic light scattering (DLS) studies to investigate the equilibrium conformational structure of single-phase polymer−SCF solutions.[13−16] Also, kinetic studies of polymer−SCF solution phase separation are also being pursued.[17−21]

In a phase separation experiment, an equilibrated, single-phase system is perturbed with a temperature[22] or the pressure quench[17−21] or the addition of an nonsolvent to cross the phase boundary to a final condition inside the two-phase envelop.[23,24] In this study, we investigated the gaseous antisolvent-induced phase separation (GAS) on polymer solution. In GAS, a compressed gas is added to a polymer solution to cause a phase split into a polymer-rich phase of high concentration and polymer-lean phase that essentially does not contain any polymer. This process is a powerful tool for solvent recovery in solution polymerization process for molecular weight fractionation or separation of polymers.[25] The structure changes and correlation length of the polymer that accompany this shift of solvent are very important for the final polymer structure but not completely understood. In previous papers, we have studied the antisolvent CO_2 pressure dependence of the radius of gyration, R_g, and the second virial coefficient, A_2, in dilute solution of polystyrene (PS) in "good" solvent of tetrahydrofuran and toluene using small-angle X-ray scattering and viscosity.[26,27] We found that the R_g and A_2 decrease with increases in pressure of CO_2 because the interaction of polymer with solvent becomes weaker in this process, and these results correlate quite well with the molecular thermodynamic of polymer solution. In the present work, we make further study to the structure and properties of monodisperse polystyrene (PS) in mixed solvent of cyclohexane (CH), the Θ solvent for PS at 34.5 °C, and carbon dioxide (CO_2) at different pressures with different chemical potentials using synchrotron SAXS with high-intensity X-ray beams whose incident wavelength is known with great precision. In combination with multidetectors, this permits measurements of high signal-to-noise ratio to be made at relatively short time.

* To whom correspondence should be addressed: e-mail hanbx@pplas.icas.ac.cn; Tel 86-10-62562821; Fax 86-10-62559373.

10.1021/ma021293e CCC: $22.00
Published on Web 11/27/2002

Experimental Section

Materials. Monodisperse polystyrene (PS) ($M_w/M_n \leq 1.08$) was synthesized by Nanjing Chemical Engineering University. The molecular weight information of the polymer is shown in Table 1. The solvent cyclohexane (CH) was purchased from Beijing Chemical Factory (>99.5%) and used as received. Each PS sample was dissolved in CH in a vial at room temperature for more than 48 h before the experiments. Complete dissolution of the polymer was confirmed by observing transparency of the solution. The solution concentrations were 4.60×10^{-4}, 6.88×10^{-4},1.08×10^{-3}, 3.51×10^{-3}, and 9.19×10^{-3} g/cm^3.

Phase Behavior. The procedure and apparatus for phase behavior study are similar to our previously study.[26,27] Briefly, a suitable amount of PS/CH solution was loaded into optical cell with volume of about 30 mL and two sapphire windows for observing the phase behavior directly. After removing the air, the CO_2 was charged into the cell by a high-pressure syringe pump. The volume expansion of the solution at different CO_2 pressures could be known from the graduations on the cell. The cloud-point pressure (P_c), which is defined as the pressure at which the solution becomes supersaturated and the polymer begin to precipitate, was obtained from observation. Each cloud point is reproduced three or four times at each concentration of the solution with a scatter of approximately ±1.0 bar.

Small-Angle X-ray Scattering. The high-pressure SAXS cell consisted mainly of a stainless steel body and two diamond windows of 8 mm diameter and 0.4 mm thickness. The SAXS path length was fixed at 1.5 mm. The cell had a volume of 2.7 cm^3 and has a maximum pressure rating of 200 bar. The CO_2 pressure was monitored to ±0.25 bar in the pressure range of 0−200 bar using an electrical transducer (FOX-BORO/ICT). The temperature of the cell was controlled to ±0.1 K using a platinum resistance temperature probe (model XMT, produced by Beijing Chaoyang Automatic Instrument Factory).[26,27]In a typical experiment, a suitable amount of PS/CH solution was loaded into the SAXS cell. The cell was maintained at 34.5 °C, and CO_2 was slowly charged with stirring. The pressure was controlled carefully using the valve on the cell. The system was equilibrated at the fixed temperature and pressure. The SAXS measurement was conducted after equilibrium had been reached.

Synchrotron SAXS measurements were performed at Beamline 4B9A at Beijing Synchrotron Radiation Facility,[28] using a SAXS apparatus constructed at the station over q ranges of $0.005 < q$ (Å) < 0.15, where $q = 4\pi \sin(\vartheta/2)/\lambda$, with θ and λ being respectively the scattering angle and incident X-ray wavelength of 1.54 Å. The data accumulation time was roughly 10 min for each condition, which depended on the intensity of incident X-ray. The distance between the sample chamber and detector was 1.52 m. During the experiment, the intensity of the incident beam was measured by a counter positioned upstream from the cell. The transmission through the cell was determined from measurements made by upstream and downstream ionization monitors. Prior to comparison, the results from separate experiments made under different sample and different instrument conditions were scaled to remove difference due to nonuniformity, beam intensity, and sample transmission. The useful intersities are those scattered by the sample $I_S(q)$ and by a reference sample $I_r(q)$ used in order to subtract the background. In our experiment, the scattering intensity of the mixed solvent at the same condition as the solution is used as $I_r(q)$. The attenuation factors of the sample and reference sample are respectively

$$T_s = \frac{I_s(0)}{B(0)}; \quad T_r = \frac{I_r(0)}{B(0)} \tag{1}$$

where $B(\theta)$ is the intensity registered without sample.

The subtracted intensity $I(q)$ can be obtained by

$$I(q) = \frac{I_s(q)}{T_s} - \frac{I_r(q)}{T_r} \tag{2}$$

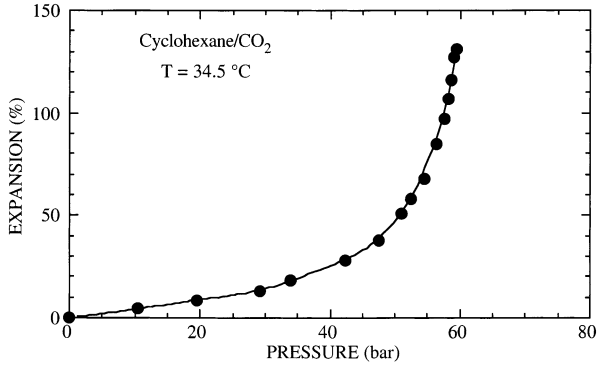

Figure 1. Volume expansion of cyclohexane by carbon dioxide at temperature of 34.5 °C.

Table 1. Molecular Weights of the Polystyrene Samples

polymer	M_w	M_n	M_w/M_n
PS-3.6K	3 600	3 500	1.03
PS-22.4K	22 400	21 300	1.05
PS-84K	84 000	79 200	1.06
PS-176K	176 000	168 000	1.05
PS-341K	341 000	316 000	1.08

The contribution to the X-ray scattering from polymer chain, $I(q)$, can arise from two sources: the particle contribution (the particle here concerns polymer in solvent), $P(q)$, which depend solely upon the size and shape of the particles; an appropriate structure factor, $S(q)$, which accounts for attractive or repulsive interactions between particles.[29] By assuming that the solvent is structureless, the total scattering is

$$I(q) = \rho S(q)\, P(q) \tag{3}$$

where ρ is the particle number density and q is the magnitude of the scattering vector. Aggregation of the solute polymer with each other leads to the increase in the structure factor at low q; however, when the system is sufficiently dilute, interparticle interactions are significantly reduced, yielding $S(q) = 1$. In our system, the experiments were conducted at very low concentration (below the overlap concentration C^*); therefore, we can obtain the $P(q)$ directly from scattering curve at low-q range from 0.0047 to 0.01 Å using the Debye equation.[30] The intermolecular correlation length, ξ, can be determined by fitting the scattering data using Ornstein−Zernike (OZ) equation at mid-q range from 0.01 to 0.06 Å.[31]

Results and Discussion

Phase Behavior. In the GAS process for our system, CO_2 dissolves into the PS/CH solution, and when the sufficient gas is absorbed by the solution, the gas acts as an antisolvent and the PS precipitate. This process occurs with an expansion of the liquid. Figure 1 shows the expansion behavior of CH by CO_2 at 34.5 °C. It is important to determine the volumetric expansion characteristics as a function of pressure because of subsequent SAXS experiment considerations. For example, SAXS cell dimensions dictate the maximum amount of solution that can be added before it is completely filled due to expansion.

Figure 2 shows the cloud-point pressure (P_c) of the PS + CH + CO_2 ternary system with different molecular weight (M_w) of PS and solution concentrations at temperature of 34.5 °C. P_c increases with decreasing concentration and M_w of the polymer. According to molecular thermodynamics, the solubility of the polymer in solvent depends on the Gibbs free energy ΔG_m, which is a function of enthalpy of mixing ΔH_m and entropy of mixing ΔS_m. ΔH_m depends on solution density and on the strength of polymer segment−segment, solvent−

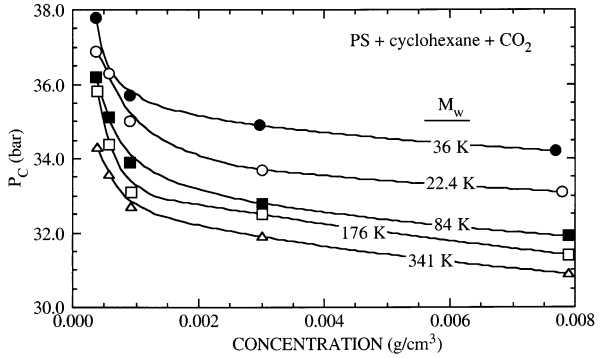

Figure 2. Effect of molecular weight and concentraion of polystyrene (PS) in cyclohexane on the cloud-point pressure (P_c) at temperature of 34.5 °C.

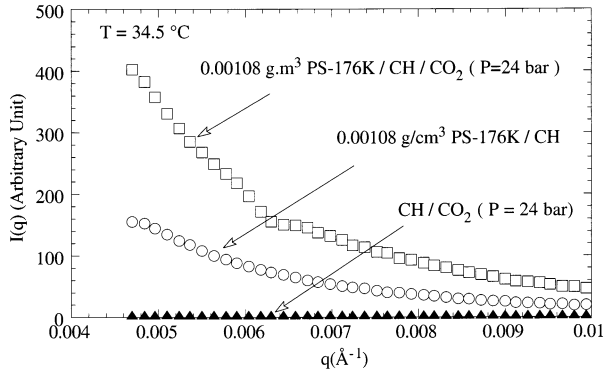

Figure 3. SAXS scattering data for mixed solvent of cyclohexane/CO_2 (P = 24 bar), 0.001 08 g/cm^3 PS-176K/cyclohexane solution, and the same solution added with CO_2 (P = 24 bar) at 34.5 °C in the low-q range from 0.0047 to 0.01 Å^{-1}.

solvent, and polymer segment−solvent interactions. ΔS_m depends on both the combinatorial entropy of mixing and the noncombinatorial contribution associated with the volume change on mixing.[32] In the course of the adding CO_2, the interaction between the CH and CO_2 weakens the interaction between PS and CH, which causes the increasing in polymer−polymer interaction, and PS precipitates from the solution at certain CO_2 pressure. The interaction between solvent and antisolvent is the dominant factor for this process. The phase behavior of Figures 1 and 2 are the basis for the following SAXS experiment, in which the CO_2 pressures had been chosen to make sure the polymer did not precipitate from the solution.

Small-Angle X-ray Scattering. We did SAXS experiments for five PS samples and each at four different solution concentrations. For every sample and concentration, six different CO_2 pressures of 0, 6, 12, 18, 24, and 30 bar have been measured. As an example, Figure 3 compares the scattering of the 0.001 08 g/cm^3 PS-176K/CH solution, PS-176K/CH/CO_2 (P = 24 bar) mixture, and accordingly the CH/CO_2 (P = 24 bar) mixed solvent. The mixed solvent displays very low background scattering since it is structureless. The source of the scattering in the PS/CH solution is due to differences in the electron density of the electron-rich, highly aromatic polymer chain and the electron-poor solvent. Dilution with antisolvent CO_2 causes a large increase in the scattering at the low-q range due to the reduction in the electron density of the solvent phase, providing better contrast between the polymer and solvent, and an increase in the PS attractive interactions shown as an increase in the structure factor $S(q)$ in eq 3.

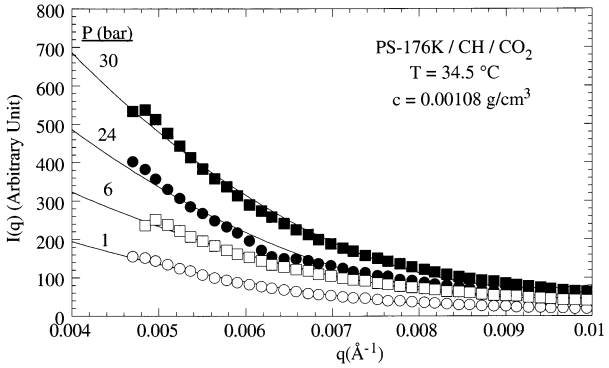

Figure 4. Effect of pressure of CO_2 on the SAXS scattering of 0.001 08 g/cm^2 PS-176K/cyclohexane solution at temperature of 34.5 °C. The smooth curves are fits of the Debye equation.

Table 2. Radius of Gyration, R_g, Values Obtained from the Debye Equation

CO_2 press. (bar)	radius of gyration, R_g (Å)				
	PS-3.6K	PS-22.4K	PS-84K	PS-176K	PS-341K
0.0	16.1	40.1	77.7	112.4	156.5
6.0	15.6	37.0	69.3	98.4	134.6
12.0	14.4	32.3	58.0	80.5	107.9
18.0	13.1	27.9	48.1	65.2	85.6
24.0	12.9	25.9	42.9	56.8	73.1
30.0	10.8	20.1	31.6	40.6	50.8

The effect of CO_2 pressure on scattering of X-rays from the above solution is shown in Figure 4. As the pressure increases, the scattering at low-q range increases appreciably. Such behavior can be attributed to the aggregation of the polymer chain due to the increase of polymer−polymer interaction. This also means that the $S(q)$ in eq 3 increases and the $I(q)$ increases. This phenomenon was observed for PS in other organic solvent studied before.[26,27]

The intramolecular correlation defined by R_g at different antisolvent pressure for different concentration of the solution is determined by Debye equation at low q scattering range. For the random coil, the form factor is given by the Debye function as[30]

$$P(q) = \frac{2}{q^4 R_g^4}[\exp(-q^2 R_g^2) + q^2 R_g^2 - 1] \qquad (4)$$

Then the R_g at different CO_2 pressures for different M_w of PS was determined by extrapolation the R_g at different concentrations to zero concentration. The R_g values obtained are listed in Table 2. Figure 5 also compares the values of R_g as the critical pressure is approached isothermally for different M_w. The R_g values obtained at each M_w without antisolvent CO_2 are in excellent agreement with the unperturbed θ value for PS in CH obtained from the power low relationship, $R_{g-\theta} \approx 0.269 M_w^{0.5}$.[33−35] With the increasing of the pressure of CO_2, the R_g decreases, which means the polymer aggregate in the process of approaching the phase separation boundary. CH is the Θ solvent for PS at 34.5 °C, and PS coil is expanded due to prevailing intersegmental repulsion; with the adding of antisolvent, the solvent power of CH is reduced and PS chain is shrink due to prevailing intersegmental attraction, which induce PS chain collapse, overlap, and entanglement. This phenomenon was also observed for PS in THF[26] and PS in toluene.[27] The effect of M_w on R_g at different

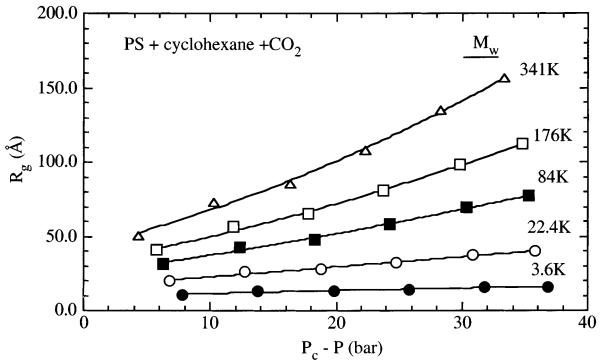

Figure 5. Changes in radius of gyration R_g for PS in cyclohexane/CO_2 mixed solvents at temperature of 34.5 °C as a function of pressure distance to cloud point. The P_c in the figure is the cloud-point pressure, and the P is the experiment pressure.

Table 3. Correlation Length, ξ, Values Obtained from the Ornstein−Zernike Equation

CO_2 press. (bar)	correlation length, ξ (Å)				
	PS-3.6K	PS-22.4K	PS-84K	PS-176K	PS-341K
0.0	9.3	23.2	44.8	64.9	90.4
6.0	15.6	35.2	54.9	78.1	111.2
12.0	25.7	55.3	79.2	95.2	123.9
18.0	43.2	79.6	105.2	125.2	147.8
24.0	60.9	110.1	140.2	180.9	238.3
30.0	80.2	150.2	200.3	270.3	361.7

CO_2 pressure can be extracted from Figure 5. If the values of R_g are replotted double-logarithmically against M_w at different CO_2 pressures, the data point can be fitted by straight line with following power law relationships:

$$R_g = 0.268M_w^{0.5} \quad (T = 34.5\ °C, P = 0\ \text{bar}) \quad (5)$$

$$R_g = 0.321M_w^{0.474} \quad (T = 34.5\ °C, P = 6\ \text{bar}) \quad (6)$$

$$R_g = 0.382M_w^{0.443} \quad (T = 34.5\ °C, P = 12\ \text{bar}) \quad (7)$$

$$R_g = 0.450M_w^{0.412} \quad (T = 34.5\ °C, P = 18\ \text{bar}) \quad (8)$$

$$R_g = 0.570M_w^{0.381} \quad (T = 34.5\ °C, P = 24\ \text{bar}) \quad (9)$$

$$R_g = 0.662M_w^{0.341} \quad (T = 34.5\ °C, P = 30\ \text{bar}) \quad (10)$$

From the exponential relationship above, we find the exponents are decreasing from 0.5 to 0.341, which means that the shape of the PS chain is changing from random coil to nearly globular with pressure approaching phase separation boundary, since the value of $^1/_3$ was predicted for globular particles by theory.[36]

A better indication of the solvent strength as a function of antisolvent CO_2 pressure is provided by intermolecular correlation length, ξ, which was obtained by Ornstein−Zernike (OZ) fitting at low to mid-q range of 0.0047−0.06 Å.[31]

$$S(q) = \frac{S(0)}{1 + q^2\xi^2} \quad (11)$$

The values of ξ at different CO_2 pressures are listed in Table 3. Correlating the $R_{g-\theta}$ listed in Table 2 and $\xi_{T\theta}$ listed in Table 3 at CO_2 pressure of 0 bar at θ temperature of 34.5 °C, the relationship of

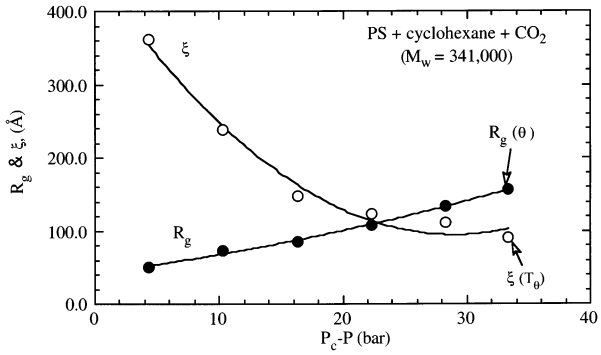

Figure 6. Changes in radius of gyrarion, R_g, and intermolecular correlation length, ξ, for PS-341K in mixed solvent of cyclohexane/CO_2 as a function of pressure distance to the cloud pressure at temperature of 34.5 °C.

$\xi_{T\theta} = R_{g-\theta}/3^{1/2}$ can be obtained, which is exactly the same as the results obtained by Melnichenko et al.,[37] Fujita et al.,[38] and Des Cloraeaus and Janink et al.[39] As an example, Figure 6 shows the behavior of ξ and R_g as a function of distance from cloud pressure for sample PS-341K. The ξ, which is a measure of the spatial extent and temporal lifetime of transient, unstable concentration fluctuations of polymer in solutions, is small in the θ region but increases dramatically near the cloud point where it is 7 times the chain dimensions ($\xi \gg R_g$), and the system exhibits antisolvent-induced phase separation. The concentration fluctuations are initiated with internal energy (k_BT) and dissipate because of the energetic penalty associated with maintaining a region of high concentration relative to more dilute surroundings. The phase separation occurs as the pressure approaches cloud point pressure. The decrease in the system's thermodynamic stability results in an increase in the size and lifetime of transient concentration fluctuation. The diverging thermodynamic fluctuations in the phase separation region lead to the formation of distinct microdomains, representing interpenetrating of macromolecules and dramatic increase of the intermolecular correlation length.

Conclusion

The synchrotron small-angle X-ray scattering technique has been used to study the antisolvent CO_2 induced thermodynamic changing in polymer solution of polystyrene in Θ solvent of cyclohexane. The intramolecular correlation of the polymer chain decreases with the system approaching the phase separation boundary and its shape change from random coil to nearly globular from the exponential relationship between the R_g and M_w at different antisolvent pressures. The correlation lengths between the polymer chain increase with the system approaching the phase separation boundary, and it increases dramatically near the phase separation boundary.

Acknowledgment. The authors are grateful to the National Natural Science Foundation of China (20133030).

References and Notes

(1) Maillols, H.; Bardet, L.; Gromb, S. *Eur. Polym. J.* **1978**, *14*, 1015.
(2) Pouchly, J.; Zivny, A. *Makromol. Chem.* **1983**, *184*, 2081.
(3) Dondos, A.; Benoit, H. *J. Polym. Sci., Polym. Phys. Ed.* **1977**, *15*, 137.

(4) Celda, B.; Gomaz, C.; Gavara, R.; Tejero, R.; Campos, A. *Makromol. Chem*. **1987**, *188*, 2909.
(5) Munk, P.; Abijaoude, M. T.; Halbrook, M. E. *J. Polym. Sci., Polym. Phys. Ed*. **1978**, *16*, 105.
(6) Jejero, R.; Gomez, C.; Celda, B.; Gavara, R.; Campos, A. *Makromol. Chem*. **1988**, *189*, 1643.
(7) Campos, A.; Celda, B.; Tejero, R.; Figueruelo, J. E. *Eur. Polym. J*. **1984**, *20*, 447.
(8) Celda, B.; Campos, A.; Tejero, R.; Figueruelo, J. E. *Eur. Polym. J*. **1986**, *22*, 129.
(9) Chu, B. *Laser Light Scattering: Basic Principles and Practice*, 2nd ed.; Academic Press: Boston, 1991.
(10) Sperling, L. H. *Polym. Eng. Sci*. **1984**, *24*, 1.
(11) Russell, T. P. *Mater. Sci. Rep*. **1990**, *5*, 171.
(12) Luna-Bárcenas, G.; Metedith, J. C.; Sanchez, I. C.; Johnston, K. P.; Gromov, D. G.; de Pablo, J. J. *J. Chem. Phys*. **1997**, *107*, 10782.
(13) DiNoia, T. P.; Kirby, C. F.; van Zanten, J. H.; McHugh, M. A. *Macromolecules* **2000**, *33*, 6321.
(14) Melnichenko, Y. B.; Kiran, E.; Heath, K.; Salaniwal, S.; Cochran, H. D.; Stamm, M.; Van Hook, W. A.; Wignall, G. D. *Scattering from Polymers; ACS Symp. Ser*. **2000**, *739*, 317.
(15) Melnichenko, Y. B.; Kiran, E.; Heath, K.; Salaniwal S.; Cochran, H. D.; Stamm, M.; Van Hook, W. A.; Wignall, G. D. *J. Appl. Crystallogr*. **2000**, *33*, 682.
(16) Van Hook, W. A.; Wilczura, H.; Rebelo, L. P. N. *Macromolecules* **1999**, *32*, 7299.
(17) Xiang, Y.; Kiran, E. *Rev. Sci. Instrum*. **1998**, *69*, 1463.
(18) Melnichenko, Y. B.; Kiran, E.; Wignall, G. D.; Heath, K.; Salaniwal S.; Cochran, H. D.; Stamm, M. *Macromolecules* **1999**, *32*, 5344.
(19) Liu, K.; Kiran, E. *Macromolecules* **2001**, *34*, 3060.
(20) Liu, K.; Kiran, E. *J. Supercrit. Fluids* **1999**, *16*, 59.
(21) Kojima, J.; Nakeyama, Y.; Takenaka, M.; Hashimoto, T. *Rev. Sci. Instrum*. **1995**, *66*, 4066.
(22) Hashimoto, T. *Phase Transitions* **1988**, *12*, 47.
(23) Matsuyama, H.; Yamamoto, A.; Yano, H.; Maki, T.; Teramoto, M.; Mishima, K.; Matsuyama, K. *J. Membr. Sci*. **2002**, *204*, 81.
(24) Schuhmacher, E.; Soldi, V.; Pires, A. T. N. *J. Membr. Sci*. **2001**, *184*, 187.
(25) McHugh, M. A.; Krukonis, V. *Supercritical Fluid Extraction*, 2nd ed.; Butterworth-Heinemann: Boston, 1994.
(26) Li, D.; Liu, Z. M.; Han, B. X.; Yang, G. Y.; Wu, Z. H.; Liu, Y.; Dong, B. Z. *Macromolecules* **2000**, *33*, 7990.
(27) Li, D.; Han, B. X.; Liu, Z. M.; Liu, J.; Zhang, X. G.; Wang, S. G.; Zhang, X. F.; Wang, J.; Dong, B. Z. *Macromolecules* **2001**, *34*, 2195.
(28) Dong, B. Z.; Sheng, W. J.; Yang, H. L.; Zhang, Z. J. *J. Appl. Crystallogr*. **1997**, *30*, 877.
(29) Glatter, G.; Krathy, O. *Small-Angle X-ray Scattering*; Academic Press: London, 1982.
(30) Debye, P. *J. Chem. Phys*. **1946**, *14*, 636.
(31) Benoît, H.; Picot, C.; Benmouna, M. *J. Polym. Sci., Part B: Polym. Phys*. **1984**, *22*, 1545.
(32) Kirby, C. F.; McHugh, M. A. *Chem. Rev*. **1999**, *99*, 565.
(33) Lal, J.; Bansil, R. *Macromolecules* **1991**, *24*, 290.
(34) Cotton, J. P.; Decker, D.; Benoît, H.; Farnous, B.; Higgins, J.; Jannink, G.; Ober, R.; Picot, C.; Des Cloizeaus, J. *Macromolecules* **1974**, *7*, 863.
(35) Schmidt, M.; Burchard, W. *Macromolecules* **1981**, *14*, 210.
(36) Nakata, M. *Makromol. Chem*. **1971**, *149*, 99.
(37) Melnichenko, Y. B.; Wignall, G. D.; Van Hook, W. A.; Szydlowsky, J.; Wilczura, H.; Rebelo, L. P. *Macromolecules* **1998**, *31*, 8436.
(38) Fujita, H. *Polymer Solutions*; Elsevier: Amsterdam, 1990.
(39) Des Cloizeaux, J.; Jannink, G. *Polymers in Solution: Their Modeling and Structure*; Clarendon Press: Oxford, 1990.

MA021293E